

A COMPARATIVE REVIEW OF CAMERA CALIBRATING METHODS WITH ACCURACY EVALUATION¹

X. Armangué, J. Salvi and J. Batlle

Institut de Informàtica i Aplicacions

Universitat de Girona

Av. Lluís Santaló, s/n, E-17071 Girona (Spain)

Mail: {armangué, qsalvi, jbatlle}@eia.udg.es

Abstract

Camera modelling and calibrating is a crucial problem for further metric measuring of a scene. A lot of different calibrating techniques and surveys about calibration have been presented in last years. However, it is still difficult to go into details of a determined calibrating technique and to compare it with respect to the others. Mainly, this problem emerges due to the lack of notation standardization and the different existing methods of accuracy evaluation. This article presents a detailed review about five of the most used calibrating techniques and a great deal of effort has been done to present them by using the same notation. Moreover, the techniques have been implemented and the accuracy evaluation results are shown in the article.

1. INTRODUCTION

Camera calibration is the first step toward computational computer vision. Although some information from the measuring scenes can be obtained from uncalibrated cameras, calibration is essential when metric information is required. Some applications of this capability includes:

1. *Dense reconstruction*: Each image point determines an optical ray passing through the focal point of the camera toward the scene. Use of more than a view of a motionless scene permits to cross both optical rays and get the metric position of the 3D point.
2. *Visual inspection*: Once a dense reconstruction of a measuring object is obtained, it can be compared with an stored model in order to detect some manufacturing imperfections as bumps, dents and cracks.

¹This work has been supported by Spanish project CICYT TAP99-0443-C05-01.

3. *Object localization:* From points of different objects, the position relation among these objects can be easily determined, which has many application in industrial part assembly and obstacle avoidance in robot navigation, among others.
4. *Camera localization:* When a camera is placed at the hand of a robot arm or on a mobile robot, the position and orientation of the camera can be computed through the localization of some known landmarks in the scene. If these measures are stored, a temporal analysis permits to obtain the trajectory of the robot, which can be used in robot control and path planning.

Camera calibration can be classified according to several different criteria. For instance, 1) Linear versus nonlinear camera calibration (usually differentiate by the modelling or not of the lens distortion [1]). 2) Implicit versus explicit calibration. Implicit calibration is the process of calibrating a camera without explicitly computing its physical parameters. Although, the results can be used for 3D measurement and generation of image coordinates, they are useless for camera modelling as the obtained parameters do not correspond to the physical ones [2]. And 3), methods that use known 3D points as a calibrating pattern [3], and others that use some geometrical properties of the scene such as vanishing lines. Moreover, the approaches can be classified with respect to the calibrating method used to estimated the parameters of the camera model:

1. *Non linear optimization techniques.* The camera parameters are obtained through iteration with the constraint of minimizing a determined function. The advantage of these techniques is that it can calibrate nearly any model and the accuracy usually increase by increasing the number of iterations. However, these techniques require a good initial guess in order to guarantee the convergence. Examples: classic photogrammetry and Salvi [4].
2. *Linear techniques which compute the transformation matrix.* These techniques use the least squares method to obtain a transformation matrix which relates 3D points with their projections. However, these techniques can not model lens distortion. Moreover, it's sometimes difficult to extract the parameters from the matrix due to the implicit calibration used. Examples: Hall [5], Toscani-Faugeras [3] and Ito [1].
3. *Two-step techniques.* These techniques use a linear optimization to compute some of the parameters and, as a second step, the rest of parameters are iteratively computed. These techniques permit a rapid calibration reducing considerably the number of iterations. Moreover, the convergence

is nearly guarantee due to the linear guess obtained in the first step. Examples: Tsai [6], Weng [7] and Wei [2].

This article is a detailed survey of some of the most used calibrating techniques. A great deal of effort has been done to present the survey using the same notation. Moreover, the techniques have been implemented and comparative results are shown and discussed.

The article is structured as follows: Section 2 deals with camera modelling. Section 3 describes some techniques of camera calibrating. Section 4 explains some methods for the accuracy evaluation of camera calibrating techniques. The paper ends with conclusions.

2. CAMERA MODEL

The model is a mathematical formulation which approximates the behaviour of any physical device, i.e a camera. In such a case, the internal geometry and the position and orientation of the camera in the scene is modelled. There are several camera models depending on the desired accuracy. The simplest model is the one proposed by Hall [5]. The goal is to find a relationship among the 3D points of the scene with their 2D projecting point in the plane image. This relationship is approximated by means of a transformation matrix.

$$\begin{pmatrix} s^I X_d \\ s^I Y_d \\ s \end{pmatrix} = \begin{pmatrix} A_{11} & A_{12} & A_{13} & A_{14} \\ A_{21} & A_{22} & A_{23} & A_{24} \\ A_{31} & A_{32} & A_{33} & A_{34} \end{pmatrix} \begin{pmatrix} {}^w X_w \\ {}^w Y_w \\ {}^w Z_w \\ 1 \end{pmatrix} \quad (1)$$

Then, given a 3D point P_w with respect to the metric world coordinate system, applying the transformation matrix proposed by Hall, the 2D point P_u in pixels with respect to the image coordinate system is obtained. However, other more complex models decompose the transformation of the point P_w into the point P_d in 4 steps, explained in the following (see also figure 1):

1. The first step consists on relating the point P_w from the world coordinate system to the camera coordinate system.
2. Next it is necessary to carry out the projection of the point P_c on the image plane obtaining the point P_u , by using a projective transformation.
3. The third step models the lens distortion, based on a disparity of the real projection. Then, the point P_u is transformed to the real projection P_d .
4. Finally, the last step consists on carrying out another coordinate system transformation in order to go from the metric coordinate system of the camera to the image coordinate system of the computer in pixels.

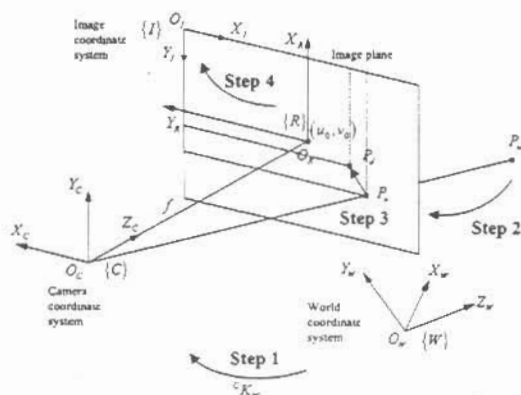


Figure 1: The geometric relation between a 3D point and its 2D projection.

In the following four different camera models (Faugeras-Toscani [3], Faugeras-Toscani with distortion [4], Tsai [6] and Weng [7]) are explained in detail considering how they carry out this four steps.

2.1. Changing from the world to the camera coordinate system

Changing the system of coordinates of the world to the system of coordinates of the camera is carried out in the same way in the 4 surveyed models. This transformation is modelled using a translation vector and a rotation matrix,

$$\begin{pmatrix} {}^c X_w \\ {}^c Y_w \\ {}^c Z_w \end{pmatrix} = {}^c R_W \begin{pmatrix} {}^w X_w \\ {}^w Y_w \\ {}^w Z_w \end{pmatrix} + {}^c T_W \quad (2)$$

2.2. Projection of the point 3D on the image plane

Consider that any optical sensor can be modelled as a *pinhole camera*. That is, the image plane is located at a distance f from the optical centre O_c , and it is parallel to the plane defined by the coordinate axis X_c and Y_c . Moreover, given an object point P_w related to the camera coordinate system, if it is projected through the focal point O_c , the optical ray intercepts the image plane at the 2D image point P_u . This relation is shown in equation. The four reviewed models solved the projective transformation by using equation (3).

$${}^c X_u = f \frac{{}^c X_w}{{}^c Z_w} \quad {}^c Y_u = f \frac{{}^c Y_w}{{}^c Z_w} \quad (3)$$

2.3. Lens distortion

The third step is based on modelling of the distortion of the lenses. Each surveyed model proposed different approaches. Equation (4) transforms the point P_u without distortion to the point P_d with distortion, δ_x and δ_y represents the applied distortion.

$${}^C X_u = {}^C X_d + \delta_x \quad {}^C Y_u = {}^C Y_d + \delta_y \quad (4)$$

The camera model proposed by Faugeras-Toscani [3] does not model the lens distortion, therefore P_u and P_d are the same point. In this case δ_x and δ_y are zero.

The model of Faugeras-Toscani can be improved by modelling the lens distortion [4] as also considered Tsai [6]. This displacement can be modelled by equation (5), which considers only the first coefficient k_1 .

$$\delta_x = k_1 {}^C X_d \left({}^C X_d^2 + {}^C Y_d^2 \right) \quad \delta_y = k_1 {}^C Y_d \left({}^C X_d^2 + {}^C Y_d^2 \right) \quad (5)$$

The model of Weng [7] considers three types of distortion: radial distortion, decentering distortion and thin prism distortion. The total distortion will be the sum of the three distortions like it is shown in the following equations,

$$\delta_x = \delta_{xr} + \delta_{xd} + \delta_{xp} \quad \delta_y = \delta_{yr} + \delta_{yd} + \delta_{yp} \quad (6)$$

The radial distortion is modelled in the same way Tsai did. The decentering distortion is due to that the optic centre of the lenses is not correctly aligned with the centre of the camera [7]. This type of distortion introduces a radial and tangential distortion. Moreover, the thin prism distortion arises from imperfection in lens design and manufacturing as well camera assembly. This type of distortion can be modelled adding a thin prism in the optic system, causing radial and tangential distortions [7]. Adding the three types of distortions the following equations are obtained,

$$\begin{aligned} \delta_x &= (g_1 + g_3) {}^C X_d^2 + g_4 {}^C X_d {}^C Y_d + g_1 {}^C Y_d^2 + k_1 {}^C X_d \left({}^C X_d^2 + {}^C Y_d^2 \right) \\ \delta_y &= g_2 {}^C X_d^2 + g_3 {}^C X_d {}^C Y_d + (g_2 + g_4) {}^C Y_d^2 + k_1 {}^C Y_d \left({}^C X_d^2 + {}^C Y_d^2 \right) \end{aligned} \quad (7)$$

2.4. Changing from the camera to the computer image coordinate system

The last step deals with relating the P_d point with respect to the computer image plane in pixels. This change of coordinates can be made in two different ways according to the surveyed camera models.

The camera models proposed by Faugeras-Toscani, Faugeras-Toscani with distortion and Weng use the following equations,

$${}^I X_d = -k_u {}^C X_d + u_0 \quad {}^I Y_d = -k_v {}^C Y_d + v_0 \quad (8)$$

where, (k_v, k_u) are these parameters transforms from metric measures with respect to the camera coordinate system to pixels with respect to the computer image coordinate system; and (u_0, v_0) are these components defines the projection of the focal point in the plane image in pixels, i.e. the principal point.

The camera model of Tsai proposed another equations to carry out the same transformation. The equations are the following,

$${}^I X_d = s_x d'_x {}^{-1} {}^C X_d + u_0 \quad {}^I Y_d = d'_y {}^{-1} {}^C Y_d + v_0 \quad (9)$$

where, (u_0, v_0) are the coordinates of the projection of the focal point in the plane image in pixels; s_x is the image scale factor; d_x is the centre to centre distance between adjacent sensor elements in the X direction; d_y is the centre to centre distance between adjacent sensor elements in the Y direction; N_{cx} is the number of sensor elements in the X direction; N_{fx} is the number of pixels in a line as sampled by the computer; and $d'_x = d_x \frac{N_{fx}}{N_{cx}}$.

3. CALIBRATING METHODS

The calibrating method depends on the model used to approximate the behaviour of the camera. The linear models, i.e Hall and Faugeras-Toscani, use a least-squares technique to obtain the parameters of the model. However, non-linear calibrating methods as: Faugeras-Toscani with distortion, Tsai and Weng; use a two stages technique. They carry out a linear approximation with the aim of obtaining an initial guess for a further iterative optimization.

3.1. Method of Hall

The method used to calibrate the model of Hall is based on expressing equation (1) in the following form,

$$\begin{aligned} {}^I X_u &= \frac{A_{11} {}^W X_w + A_{12} {}^W Y_w + A_{13} {}^W Z_w + A_{14}}{A_{31} {}^W X_w + A_{32} {}^W Y_w + A_{33} {}^W Z_w + A_{34}} \\ {}^I Y_u &= \frac{A_{21} {}^W X_w + A_{22} {}^W Y_w + A_{23} {}^W Z_w + A_{24}}{A_{31} {}^W X_w + A_{32} {}^W Y_w + A_{33} {}^W Z_w + A_{34}} \end{aligned} \quad (10)$$

Then, consider that the 3D position of a set of n calibrating points and their corresponding 2D projection in the image are known (n should be bigger or equal to 6). Moreover, if we consider without lost of generality that $A_{34} = 1$, all the elements of the transformation matrix A can be obtained by using a linear least-squares technique as the pseudo-inverse [5].

3.2. Method of Faugeras-Toscani

In order to obtain the complete model of the camera, it is necessary to combine equations (2), (3), (4) and (8), obtaining (11).

$$\begin{aligned} {}^I X_u &= -k_u f \frac{r_{11}^w X_w + r_{12}^w Y_w + r_{13}^w Z_w + t_x}{r_{31}^w X_w + r_{32}^w Y_w + r_{33}^w Z_w + t_z} + u_0 \\ {}^I Y_u &= -k_v f \frac{r_{21}^w X_w + r_{22}^w Y_w + r_{23}^w Z_w + t_y}{r_{31}^w X_w + r_{32}^w Y_w + r_{33}^w Z_w + t_z} + v_0 \end{aligned} \quad (11)$$

Note that equation (11) can be expressed in matricial form in the following way, where $\alpha_u = -fk_u$ and $\alpha_v = -fk_v$.

$$\begin{pmatrix} s^I X_d \\ s^I Y_d \\ s \end{pmatrix} = \begin{pmatrix} \alpha_u r_1 + u_0 r_3 & \alpha_u t_x + u_0 t_z \\ \alpha_v r_2 + v_0 r_3 & \alpha_v t_y + v_0 t_z \\ r_3 & t_z \end{pmatrix} \begin{pmatrix} {}^w X_w \\ {}^w Y_w \\ {}^w Z_w \\ 1 \end{pmatrix} \quad (12)$$

Then, equation (12) is combined in the following way,

$$\begin{aligned} {}^I X_u &= \frac{A_1}{A_{34}} {}^w P_w + \frac{A_{14}}{A_{34}} - \frac{A_3}{A_{34}} {}^w P_w {}^I X_u \\ {}^I Y_u &= \frac{A_2}{A_{34}} {}^w P_w + \frac{A_{24}}{A_{34}} - \frac{A_3}{A_{34}} {}^w P_w {}^I Y_u \end{aligned} \quad (13)$$

At that time, a set of 5 parameters are considered $X = (T_1, T_2, T_3, C_1, C_2)^T$, which are $T_1 = \frac{A_1}{A_{34}}$, $T_2 = \frac{A_2}{A_{34}}$, $T_3 = \frac{A_3}{A_{34}}$, $C_1 = \frac{A_{14}}{A_{34}}$ and $C_2 = \frac{A_{24}}{A_{34}}$. Then, the value of the vector X is obtained by using a linear least-squares technique. Finally, the camera parameters are extracted from X by using equation (12).

3.3. Method of Faugeras-Toscani with radial distortion

When a good accuracy is necessary, the linear method of Faugeras-Toscani becomes useless. However, it can be easily modified including the radial lens distortion as it has been shown in section 2.3. Nevertheless, the equations turns into non-linear and the least-squares techniques has to be replaced by an iterative algorithm.

Note that combining equation (2), (3), (4) and (5), equation (14) is obtained. Moreover, equation (8) has to be used to transform from metric coordinates to pixels.

$$\begin{aligned} {}^C X_d + {}^C X_d k_1 r^2 &= f \frac{r_{11}^w X_w + r_{12}^w Y_w + r_{13}^w Z_w + t_x}{r_{31}^w X_w + r_{32}^w Y_w + r_{33}^w Z_w + t_z} \\ {}^C Y_d + {}^C Y_d k_1 r^2 &= f \frac{r_{21}^w X_w + r_{22}^w Y_w + r_{23}^w Z_w + t_y}{r_{31}^w X_w + r_{32}^w Y_w + r_{33}^w Z_w + t_z} \\ r &= \sqrt{{}^C X_d^2 + {}^C Y_d^2} \end{aligned} \quad (14)$$

where $x = (\alpha, \beta, \gamma, t_x, t_y, t_z, k_u, k_v, u_0, v_0, k_1)^T$ is the vector of unknowns which can be computed by using an iterative method as, for instance, the method of Newton-Raphson or Levenberg-Marquardt, among others.

Note that one of the problems of convergence in iterative algorithms is the initial guess. However, an initial guess can be obtained calibrating the linear method of Faugeras-Toscani without lens distortion, and assuming $k_1 = 0$.

3.4. Method of Tsai

The non-linear method of Faugeras-Toscani is based on fixing the initial guess without considering lens distortion. Moreover, a large number of iterations is usually necessary to obtain an accurate value of the camera parameters. The method of Tsai [6] models also the radial lens distortion but assumes that there are some parameters of the camera that are distributed by manufacturers. This fact reduces the number of calibrating parameters in the first steps. However, all of them are iteratively optimized in the last step.

Firstly, by combining equation (2), (3), (4) and (5), equation (14) is obtained. Note that, at this point Tsai's model is equivalent to the previous one of Faugeras-Toscani with distortion. Note also, that the points have been expressed in metric coordinates instead of pixels for easier comprehension (use equation (9) to express the points in pixels)

Once ${}^C X_d$ and ${}^C Y_d$ are obtained in metric coordinates by using equation (9), they can be expressed in pixels ${}^I X_d$ and ${}^I Y_d$, assuming that $s_x = 1$ and the principal point is located in the physical centre of the image plane. Moreover, by using equation (14) and considering a radial lens distortion, some geometrical principles can be applied, which leads us to the following substitution of unknowns.

$$\begin{aligned} a_1 &= t_y^{-1} s_x r_{11} & a_5 &= t_y^{-1} r_{21} \\ a_2 &= t_y^{-1} s_x r_{12} & a_6 &= t_y^{-1} r_{22} \\ a_3 &= t_y^{-1} s_x r_{13} & a_7 &= t_y^{-1} r_{23} \end{aligned} \quad (15)$$

The a_i unknowns are obtained by using least-squares technique. Moreover, assuming that the orientation vectors of a rotation matrix are orthogonal, t_y , t_x and ${}^C R_W$ are obtained. This complete the first three steps of the method of Tsai. However, two more steps are programmed in order to calculate f , t_z and k_1 . Firstly, f , t_z are approximated by least-squares, considering $k_1 = 0$. Then, this approximation determines an initial guess, which is used by an iterative algorithm to obtain f , t_z and k_1 accurately. Finally, all the parameters are optimized iteratively with the aim of obtaining an accurate solution.

3.5. Method of Weng

The method of Tsai is based on modelling radial lens distortion. The accuracy obtained by Tsai is very good and enough for most of the applications. However, in some cases where the lens of the camera need to be accurately modelled a simple radial approximation is not enough. Weng [7] improves the

model proposed by Faugeras-Toscani [3] including three types of lens distortion as it is explained in section 2.3. Then, by using equations (2), (3), (4) and (7), equation (16) is obtained. As in the previous models, the 2D point coordinates are expressed in metric (use equation (8) to transform them to pixels).

$$\begin{aligned} f \frac{r_{11}^W X_w + r_{12}^W Y_w + r_{13}^W Z_w + t_x}{r_{31}^W X_w + r_{32}^W Y_w + r_{33}^W Z_w + t_z} &= {}^C X_d + (g_1 + g_3) {}^C X_d^2 \\ &+ g_4 {}^C X_d {}^C Y_d + g_1 {}^C Y_d^2 + k_1 {}^C X_d ({}^C X_d^2 + {}^C Y_d^2) \\ f \frac{r_{21}^W X_w + r_{22}^W Y_w + r_{23}^W Z_w + t_y}{r_{31}^W X_w + r_{32}^W Y_w + r_{33}^W Z_w + t_z} &= {}^C Y_d + g_2 {}^C X_d^2 \\ &+ g_3 {}^C X_d {}^C Y_d + (g_2 + g_4) {}^C Y_d^2 + k_1 {}^C Y_d ({}^C X_d^2 + {}^C Y_d^2) \end{aligned} \quad (16)$$

Then, equations (17) are obtained.

$$\begin{aligned} W_1 &= \alpha_u r_1 + u_0 r_3 & w_4 &= \alpha_u t_x + u_0 t_z \\ W_2 &= \alpha_v r_2 + v_0 r_3 & w_5 &= \alpha_v t_y + v_0 t_z \\ W_3 &= r_3 & w_6 &= t_z \end{aligned} \quad (17)$$

At this point, $W = (W_1, W_2, W_3, w_4, w_5, w_6)^T$ is computed by using a linear least-squares technique. Then, w_6 is assumed to be the unity in order to extract from W the values of all the parameters of the vector $m = (u_0, v_0, \alpha_u, \alpha_v, t_x, t_y, t_z, \alpha, \beta, \gamma)^T$, without considering distortion. Furthermore, ${}^C R_W$ is recalculated in order to keep orthogonality by using eigen values, and the rest of parameters are recalculated.

Then, an iterative method is used to recalculate, for the third time, the values of m , assuming zero distortion. Finally, a two stages iterative method is used. In the first stage, the parameters of $d = (k_1, g_1, g_2, g_3, g_4)^T$ are linearly obtained by using least-squares, and the second stage computes the values of m iteratively. This stages are repeated as many times as needed depending on the desired accuracy.

4. ACCURACY EVALUATION

The systems used to evaluate the accuracy of camera calibrating methods can be classified into two groups depending on whether the accuracy is measured from the 3D or 2D points. In the following some of the most used methods of accuracy evaluation are described.

4.1. 3D Measurement

1. *3D position obtained from stereo triangulation.* First, acquire two images of a set of 3D test points whose 3D coordinates are known. Second, com-

pute the estimated 3D coordinates of the same points from their projections using the calibrated parameters. Finally, compare the discrepancy between real and estimated positions.

2. *Radius of ambiguity in the calibrating plane.* First, acquire a set of 3D test points, lying on a plane of test, whose coordinates in the world coordinate system are known. Second, for each image point use the calibrated model to back project the ray from the focal point through the 2D projection. The intersection of the optical ray with the plane of test determines a point. Then, the distance from the 3D test point to the intersecting points defines a radius of ambiguity around the 3D test point.
3. *Distance with respect to the optical ray.* This method is a generalization of the previous one. In this case, the discrepancy to be measured is the distance of the 3D test points from the optical ray generated by their projections.
4. *Normalized Stereo Calibration Error.* The array of pixels in an image is projected back to the scene so that each back-projected pixel covers a certain area of the object surface. This area indicates the uncertainty of the basic resolution at this distance. Where $({}^cX_{wi}, {}^cY_{wi}, {}^cZ_{wi})$ is the real coordinates of the i th 3D object point and $({}^c\hat{X}_{wi}, {}^c\hat{Y}_{wi}, {}^c\hat{Z}_{wi})$ is the coordinates obtained by back-projecting the pixel and intersecting it with the surface plane. See Weng [7] for detailed information. Then, it is defined the Normalized Stereo Calibration Error (NSCE) as show equation 18.

$$NSCE = \frac{1}{n} \sum_{i=1}^n \left[\frac{({}^c\hat{X}_{wi} - {}^cX_{wi})^2 + ({}^c\hat{Y}_{wi} - {}^cY_{wi})^2}{{}^c\hat{Z}_{wi}^2 (\alpha_v^{-2} + \alpha_v^2) / 12} \right]^{1/2} \quad (18)$$

4.2. 2D Measurement

1. *Accuracy of distorted image coordinates.* First, take an image of a set of 3D test points. Then, calculate the 2D position on the image plane of each 3D point, taking into account lens distortion. Accuracy is obtained measuring the discrepancy between the real 2D points and the estimated one.
2. *Accuracy of undistorted image coordinates.* First, take an image of a set of 3D test points. Then, calculate the linear projection of the 3D points on the image plane. Besides, detect the real 2D points through image segmentation and remove the distortion of lens by using the camera model. Finally, accuracy is obtained measuring the discrepancy between the linear projection and the undistorted points.

5. EXPERIMENTAL RESULTS

The five calibrating techniques have been implemented and their accuracy measured by using the following criteria: 1) Distance with respect to the optical ray; 2) Normalized Stereo Calibration Error; 3) Accuracy of distorted image coordinates; 4) Accuracy of undistorted image coordinates.

Using a set of object points proposed by Tsai². Table 1 shows the accuracy measured by using the first criteria and second criteria, respectively. Comparing the mean of the results obtained in both tables, we can see that a relationship exists among the two methods. Both methods obtained similar results if they are relatively compared that is, good calibrating algorithms obtain acceptable accuracy results not depending on the evaluation method used. Moreover, table 2 shows the results of calculating the accuracy by using the third and fourth criteria, respectively.

	3D position (mm)			NSCE	N° of iterations
	Mean	σ	Max		
Hall	0.1615	0.1028	0.5634	n/a	n/a
Faugeras	0.1811	0.1357	0.8707	0.6555	n/a
Faugeras NR ³ without distortion	0.1404	0.9412	0.0116	0.6784	20
Faugeras NR with distortion	0.0566	0.0307	0.1694	0.2042	20
Tsai	0.1236	0.0684	0.4029	0.4468	57
Tsai optimized	0.0565	0.0306	0.1578	0.2037	499
Tsai with principal point of Tsai optimized	0.0593	0.0313	0.1545	0.2137	52
Tsai optimized with principal point of Tsai optimized	0.0564	0.0305	0.1626	0.2033	355
Weng	0.0570	0.0305	0.1696	0.2064	200

Table 1: Accuracy of 3D Coordinate Measurement

	2D distorted image (pix.)			2D undistorted image (pix.)		
	Mean	σ	Max	Mean	σ	Max
Hall	0.2676	0.1979	1.2701	0.2676	0.1979	1.2701
Faugeras	0.2689	0.1997	1.2377	0.2689	0.1997	1.2377
Faugeras NR without distortion	0.2770	0.2046	1.3692	0.2770	0.2046	1.3692
Faugeras NR with distortion	0.0840	0.0458	0.2603	0.0834	0.0454	0.2561
Tsai	0.1836	0.1022	0.6082	0.1824	0.1011	0.6011
Tsai optimized	0.0838	0.0457	0.2426	0.0832	0.0453	0.2386
Tsai with principal point of Tsai optimized	0.0879	0.0466	0.2277	0.0872	0.0463	0.2268
Tsai optimized with principal point of Tsai optimized	0.0836	0.0457	0.2500	0.0830	0.0454	0.2459
Weng	0.0845	0.0455	0.2608	0.0843	0.0443	0.2584

Table 2: Accuracy of 2D Coordinate Measurement

²<http://www.cs.cmu.edu/~rgw/TsaiCode.html>³Newton-Raphson

6. CONCLUSION

This article surveys five of the most used calibrating techniques. Effort has been done to unify the notation among the five methods, so that they have been presented in a way that the reader can understand them easily. We can see that the differences among them are mainly in the step concerning the modelling of lens.

Moreover, a survey on accuracy evaluation has been done. The five methods have been implemented and their accuracy analyzed. Results show that only non-linear methods obtain a 3D accuracy smaller than 0.1 mm. with a very good standard deviation. Moreover, the accuracy on the image plane of non-linear methods is much better than linear methods. However, non-linear methods are more time-consuming than linear ones. Obviously, the results only prove something already demonstrated by authors. However, in this article the five methods have been compared among them, so that the reader can choose one or another method depending on their applications. Future work, it would be useful if they could compare the same methods by artificially including noise.

References

- [1] M. Ito, "Robot vision modelling - camera modelling and camera calibration," *Advanced Robotics*, vol. 5, no. 3, pp. 321-335, 1991.
- [2] G.-Q. Wei and S. De Ma, "Implicit and explicit camera calibration: Theory and experiments," *IEEE Transactions on Pattern Analysis and Machine Intelligence*, vol. 16, pp. 469-480, May 1994.
- [3] O. D. Faugeras and G. Toscani, "The calibration problem for stereo," *Proceedings of IEEE Computer Vision and Pattern Recognition*, pp. 15-20, 1986.
- [4] J. Salvi, J. Batlle, and E. Mouaddib, "A robust-coded pattern projection for dynamic 3D scene measurement," *Int. Journal of Pattern Recognition Letters*, vol. 19, pp. 1055-1065, September 1998.
- [5] E. L. Hall, J. B. K. Tio, C. A. McPherson, and F. A. Sadjadi, "Measuring curved surfaces for robot vision," *Computer Journal*, vol. December, pp. 42-54, 1982.
- [6] R. Y. Tsai, "A versatile camera calibration technique for high-accuracy 3D machine vision metrology using off-the-shelf TV cameras and lenses," *IEEE Int. Journal on Robotics and Automation*, vol. RA-3, pp. 323-344, August 1987.
- [7] J. Weng, P. Cohen, and M. Herniou, "Camera calibration with distortion models and accuracy evaluation," *IEEE Transactions on Pattern Analysis and Machine Intelligence*, vol. 14, pp. 965-980, October 1992.